Holographic Generation of Mathieu Beams with Electrons

James Haverstick, Benjamin J McMorran



Meeting-report

Microscopy AND Microanalysis

Holographic Generation of Mathieu Beams with Electrons

James Haverstick^{1,*} and Benjamin J. McMorran¹

¹Department of Physics, University of Oregon, Eugene, OR, United States

*Corresponding author: jhaverst@uoregon.edu

Electron vortex beams are structured orbital angular momentum (OAM) carrying electron matter waves. These have been generated using a variety of techniques including phaseplates [1] and diffracting holograms [2]. Electron beams created in transmission electron microscopes (TEMs) can be sculpted into vortex beams with different intensity distributions and quantized amounts of OAM [3]. The structure and properties of these beams show potential for use in new electron imaging techniques such as electron energy loss spectroscopy (EELS) to probe chiral plasmons and nanomagnetic materials [4].

While previously reported beams are typically circularly symmetric, there are other possible vortex beam profiles to explore. We discuss potential electron vortex beams with elliptical symmetry called Mathieu beams. Outside of electron optics, these have been generated holographically with photon lasers [5]. Here we describe the construction of phase modulating holograms and propose an experimental setup for the generation of Mathieu beams inside a TEM.

Mathieu beams are solutions to the Helmholtz equation in elliptical cylindrical coordinates that can have multiple vortices or phase singularities. They form optically invariant fields [6]. This means that the intensity profile is constant along the axis of propagation and implies important properties for applications including self-healing and non-diffracting beams [7]. Stated mathematically, this is the separability of the wavefunction into longitudinal and transverse components,

$$\psi(\eta, \xi, z) = e^{ik_z z} \times \psi_t(\eta, \xi)$$

where $\eta \in [0, 2\pi]$ and $\xi \in (0, \infty]$ are elliptical coordinates, and z is along the axis of propagation. The transverse field $\psi_t(\eta, \xi)$ for a Mathieu beam of order m is written using even and odd solutions to both Mathieu's equation and Mathieu's modified equation and their associated characteristic numbers as:

$$\psi_t(\eta, \xi) = a_m(q)Ce_m(\eta; q)ce_m(\eta; q) + ib_m(q)Se_m(\xi; q)se_m(\eta; q)$$

with q as a parameter related to the ellipticity. The value of m indicates the number of vortices as well as the number of phase rotations around these vortices. Plots of the transverse wavefunction are shown in Fig. 1. Due to the nature of these beams, their qualitative properties are invariant of physical size and as such, the scale is not discussed.

To generate the Mathieu beams, blazed holographic diffraction gratings are milled onto the surface of silicon nitride membranes. This is done with a focused ion beam (FIB) using gallium ions. The hologram pattern is calculated using phase reconstruction [8]. Fork dislocations in the center of the hologram cause the phase singularities to form [3]. The calculated profile and a final milled hologram are shown in Fig. 2. The beam is encoded into the first diffraction order and the blazed profile of the hologram emphasizes this order to reduce the signal of unwanted electrons. The hologram is placed inside the TEM, and the beam is defocused so that an electron plane wave is incident. From the resulting diffraction pattern, the first order spot has the correct phase information and needs to be isolated with an aperture.

To simulate this procedure, the effect of the holographic grating on the incident electron beam is modeled using transverse wavefunctions before and after the grating as,

$$\psi_{post}(x, y) = \psi_{incident}(x, y)e^{i\kappa d(x,y)}$$

where d(x, y) is the height of the grating and κ is a complex valued material parameter specific to the silicon nitride membrane and the wavelength of the electron beam. For silicon nitride at common TEM accelerating voltages, $Re[\kappa] \gg Im[\kappa]$. Therefore, these holograms are primarily phase modulating. Fourier transforms describe the effect of the microscope lenses, and this is used to calculate the expected diffraction pattern. Fig. 3. shows plots of the simulation results.

Mathieu beams present a class of vortex beams new to electron optics and demonstrate one example of the variety of beam profiles that are yet to be explored. As an optically invariant beam with OAM and interesting elliptical symmetry, there is potential for a wide variety of applications particularly involving EELS analysis. Diffracting hologram profiles have been generated and constructed for different orders and ellipticities. Further work is needed to realize their creation in a TEM and to demonstrate their exciting properties [9].

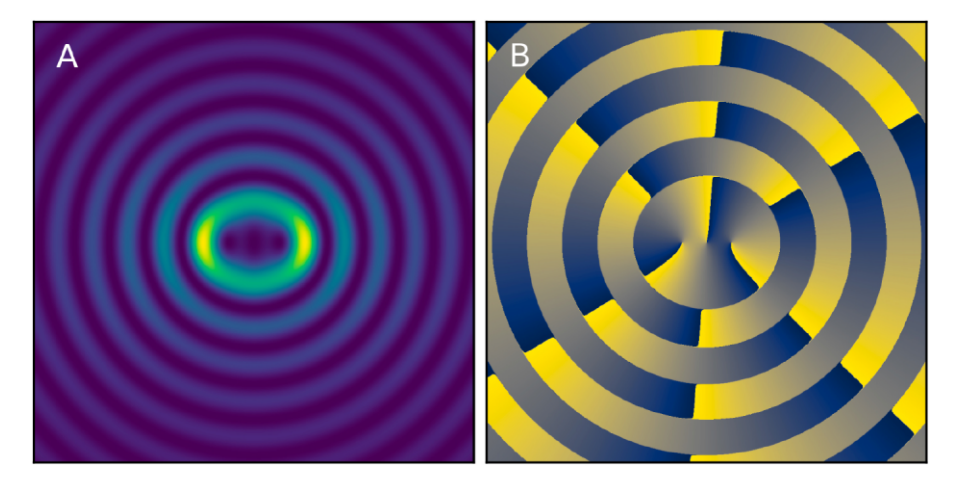


Fig. 1. A calculated Mathieu beam transverse wavefunction $\psi_t(\eta, \xi)$ for m = 3. (A) Shows the intensity $|\psi_t|^2$ and (B) shows the phase $\text{Arg}[\psi_t]$. Three vortices are shown in the center of the beam.

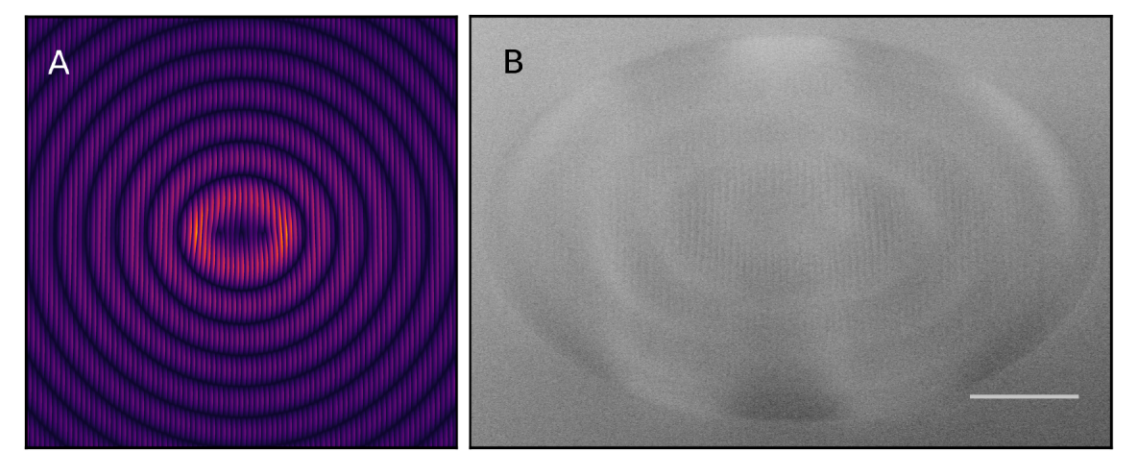


Fig. 2. (A) Simulated depth profile of a hologram for m=3 and (B) a scanning electron microscopy image of the corresponding milled grating on silicon nitride. The circular hologram is imaged at a 52° angle. The scalebar is 5 μ m, and the grating pitch is ≈ 300 nm.

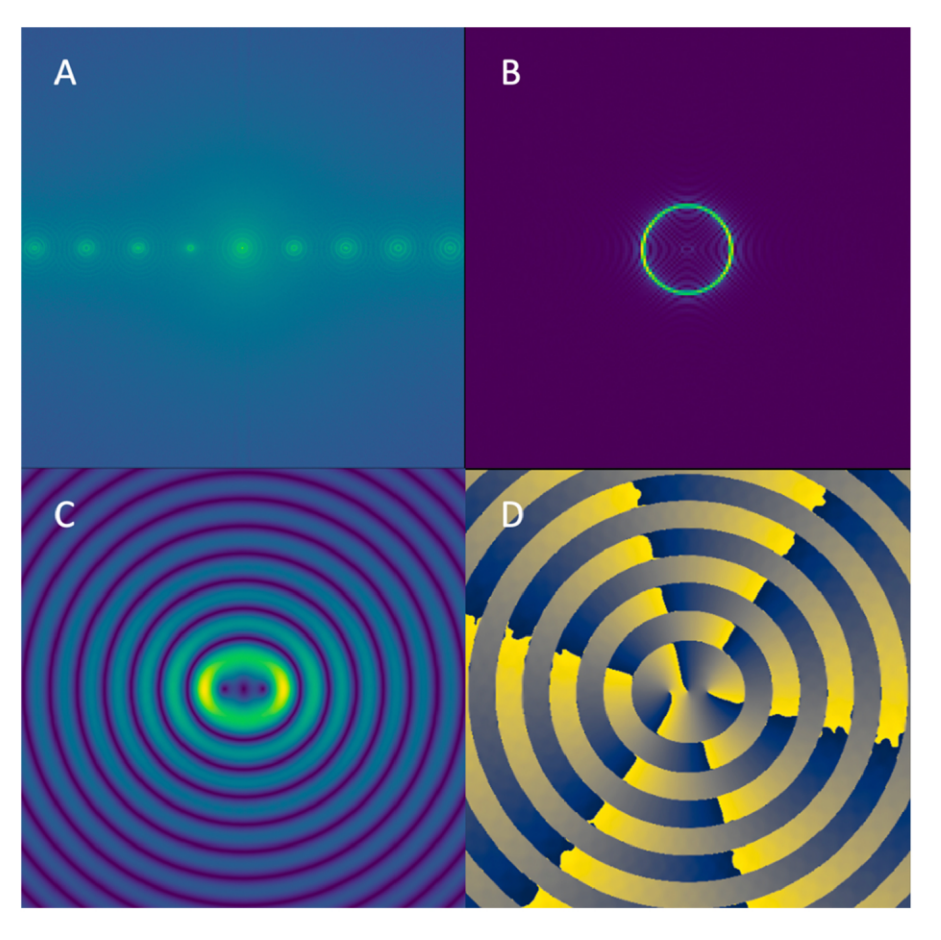


Fig. 3. (A) Simulated diffraction pattern produced by the m=3 hologram, shown with log of intensity. (B) Close up intensity of the first simulated diffraction spot. (C) Simulated intensity $|\psi_t|^2$ of the first diffraction order after being selected with an aperture. This is the desired beam. (D) The phase $\text{Arg}[\psi_t]$, corresponding to (C).

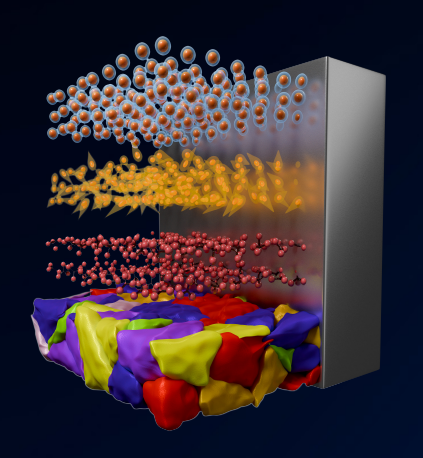
References

- 1. M Uchida and A Tonomura, Nature 464 (2010), p. 737. https://doi.org/10.1038/nature08904
- 2. J Verbeeck et al., Nature 467 (2010), p. 301. https://doi.org/10.1038/nature09366
- 3. B McMorran et al., Science 332 (2011), p. 192. https://doi.org/10.1126/science.1198804
- 4. J Verbeeck et al., CR PHYS 15 (2014), p. 190. https://doi.org/10.1016/j.crhy.2013.09.014
- 5. S Chávez-Cerda et al., Journal of Optics B: Quantum and Semiclassical Optics 4 (2002), p. S52. https://doi.org/10.1088/1464-4266/4/2/368
- 6. J Gutiérrez-Vega et al., Optics Letters 25 (2000), p. 1493. https://doi.org/10.1364/OL.25.001493
- 7. Y Ren et al., Frontiers in Physics 9 (2021), p. 1. https://doi.org/10.3389/fphy.2021.698343
- 8. C Johnson et al., Optics Express 28 (2020), p. 17334. https://doi.org/10.1364/OE.393224
- 9. This material is based upon work supported by the National Science Foundation under Grant No. 2309314.

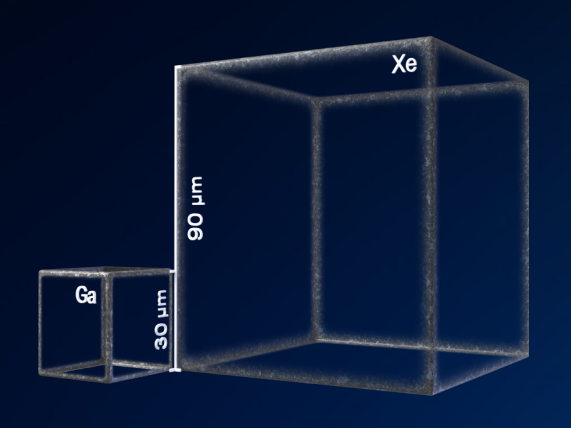


TESCANAMBER X 2

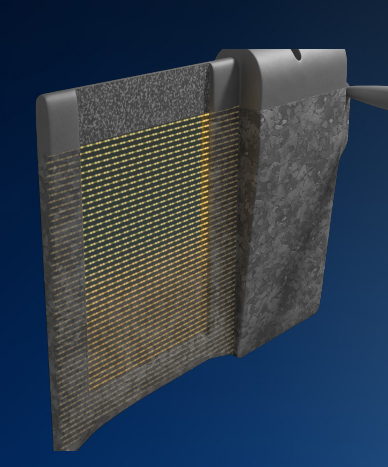
PLASMA FIB-SEM REDEFINED







SPEED REDEFINED



PRECISION REDEFINED

info.tescan.com